Consistency Testing of Lead-carbon Energy Storage Batteries Based on Random Matrix Theory and SOD

Hongchun Shu, *Member*, *IEEE*, Guangxue Wang, *Student Member*, *IEEE*, Wenlong Li, Botao Shi, and Zhongcheng Guo

***Abstract*—In this work, a consistency detection method is proposed, to overcome the inconsistencies in the use of large-scale lead-carbon energy storage batteries (LCESBs) and the difficulties of large-scale detection for LCESBs. Based on the chemical materials and physical mechanisms of LCESBs, the internal and external factors that affect the consistency and their characterization parameters are analyzed. The inconsistent characterization parameters, such as voltage, temperature, and resistance, are used to construct a high-dimensional random matrix and calculate the matrix eigenvalue. Single loop theorem and average spectral radius are then employed to carry out preliminary consistency detection. Next, short-term discharge experiments are conducted on individual batteries with inconsistent initial screening. The voltage and temperature data is collected, and sequential overlapping derivative (SOD) transformation is performed to extract the characteristics of voltage and temperature changes. The consistency of individual cells using the Wasserstein distance is quantitatively characterized. Finally, the reliability of the consistency detection method is evaluated by the confusion matrix. The large amounts of actual measurement data shows a false negative rate of the algorithm of 0 and an accuracy of 99.94%. This study shows that using random matrix theory for preliminary detection is suitable for processing high-dimensional data of large-scale energy storage power plants. Using SOD for precise detection can amplify the voltage, temperature, and resistance differences of inconsistent batteries, making the consistency detection more accurate.**

***Index Terms*—Lead-carbon batteries, consistency detection, random matrix theory, confusion matrix.**

I. Introduction

To reduce carbon emissions, the proportion of renewable energy used in the electric power grid system is gradually increasing. However, renewable energy sources have characteristics, such as low inertia and high uncertainty, and a large-scale integration can impact the stable operation of the power system. Energy storage technologies can provide a buffer to the fluctuations in the grid and support the consumption of renewable energy [1]–[3]. Lead-carbon energy storage batteries (LCESBs) possess outstanding characteristics of high efficiency, high capacity, low cost, safety, and stable large-scale configuration, thereby being widely used in new energy power stations. However, a single cell with poor consistency in a battery pack can reduce the input and output capacity, diminish the charge/discharge efficiency, and reduce the service life of the battery pack. The operational performance of the battery cluster and its service life can be improved by the timely detection of inconsistencies in individual cells and their replacement or reconstruction [4], [5].

A battery cluster is formed by connecting individual battery in series, and the performance parameters characterizing the single-cell include voltage, internal resistance, temperature, capacity, state of charge (SOC), and state of health (SOH) [6]. Reference [7] combines static and dynamic screening methods to screen retired power battery modules. Static screening can be employed to test the internal resistance and the remaining capacity of a battery module as gauge parameters for screening. The dynamic screening through SOH dynamic consistency curves can also be used for re-screening to evaluate the screening accuracy. The verification results indicate that the method can improve the screening accuracy of battery modules by at least 6.2%, laying a theoretical foundation for large-scale screening and cascading utilization of retired power batteries. This method requires a large number of SOH aging curves. Reference [8] evaluates the consistency sorting before grouping liquid metal batteries by the static and dynamic combination method. In this case, the fuzzy C-means (FCM) method is employed for

Received: January 15, 2024
Accepted: July 13, 2024
Published Online: January 1, 2025
Hongchun Shu, Guangxue Wang (corresponding author), Wenlong Li, and Botao Shi are with the State Key Laboratory Collaborative Innovation Center for Smart Grid Fault Detection, Protection and Control Jointly, Kunming University of Science and Technology, Kunming 650500, China (e-mail: kmshc@sina.com; km_wgx@163.com; kmuliwl@163.com; shibotao_kust@163.com).
Zhongcheng Guo is with the Kunming Hendera Science and Technology Co., Ltd., Kunming 650101, China (e-mail: guozhch@vip.163.com).
DOI: 10.23919/PCMP.2023.000273

static sorting and subtractive clustering for the dynamic re-sorting of discharge curves. The proposed sorting method effectively improves the consistency, weakens the "short board effect" and improves the capacity and dynamic service performance of the battery packs. The FCM clustering method has advantages in the application of consistency detection in batteries, such as more flexible clustering results, strong robustness to noise and outliers, and the ability to flexibly handle nonlinear data. However, FCM is sensitive to the initial values, has high computational complexity, and imposes high requirements for data distribution. Reference [9] uses electrochemical impedance spectroscopy to study the soft clustering of retired lithium-ion batteries. This method improves the accuracy of clustering results and the flexibility of battery recombination, giving the recombined batteries good consistency. However, electrochemical impedance spectroscopy testing is required before clustering, and the testing program is complex, making it unsuitable for practical applications. Reference [10] considers the problem of selecting retired batteries as an unsupervised clustering problem. They combines fast pulse testing with an improved split K-means algorithm to shorten the feature generation time from hours to minutes and improve the consistency detection accuracy. However, using K-means for consistency detection requires specifying the number of clusters in advance, and has weak resistance to noise and outliers. Reference [11] proposes a multi parameter evaluation method for battery consistency detection based on principal component analysis (PCA), which provided theoretical and practical basis for the consistency estimation of electric vehicle batteries. The PCA method has advantages, such as good dimensionality reduction effect, strong feature extraction ability, simple and fast algorithm in the application of consistency detection in energy storage batteries. However, it also has shortcomings, such as its dependence on linear relationships, information loss, and easily affected by outliers.

Current battery consistency testing methods mainly focus on the cascade utilization of lithium-ion batteries and group screening of liquid metal batteries. For LCESBs, existing methods cannot be used due to the differences in the composition of the materials, chemical reactions, and working environments. Therefore, developing novel methods to test the consistency of LCESBs is important. Inconsistent LCESBs can result from internal and external factors. The internal factors mainly include the influence of the material composition, production process, and chemical reaction on the electric resistance. The external factors mainly include the impact of the working environment and applied current on the battery temperature. In addition to resistance and temperature, voltage plays an important role in battery consistency.

In this study, the voltage, resistance, and temperature are extracted to construct a high-dimensional random matrix and calculate the linear eigenvalue. The single loop theorem and average spectral radius are employed to carry out the initial consistency testing of the LCESBs. Then, short-term discharge experiments on batteries are conducted to initially detect inconsistencies. The voltage and temperature data are collected, and the sequential overlapping derivative (SOD) transformation, combined with the Wasserstein distance, is utilized to accurately detect the battery consistency. The reliability of the algorithm is verified by the confusion matrix. The 0.5 MW/2 MWh LCESBs system, configured in the photovoltaic, energy storage, and charging pile integrated construction project of Kunming Hendera Science and Technology Co., Ltd., is used. A consistency algorithm is validated with an accuracy rate of 99.94% and a false negative rate of 0. Compared with the accuracy and false negative rate of the PCA, K-means, and FCM, this algorithm helps to avoid missed detections, reduce false detections, and improve the accuracy and reliability of consistency detection. Therefore, the utilization of high-dimensional random matrix preliminary detection combined with cross overlapping differential multi parameter accurate detection can improve the consistency detection accuracy of energy storage batteries, rendering it suitable for large-scale energy storage systems.

The remainder of this paper is organized as follows. Section II analyzes the representation parameters of battery inconsistencies. Section III introduces random matrix theory and its mechanism for the preliminary screening of battery inconsistencies. Section IV discusses SOD and its mechanism for the precise screening of battery inconsistencies. Section V presents a reliability evaluation model for the consistency detection algorithm. Section VI validates the accuracy of the method using actual data. Section VII presents the main conclusions of this paper.

II. Analysis of Consistency Characterization Parameters of Lead-carbon Batteries

A schematic of the functioning of the LCESB is shown in Fig.1 [12]. Carbon materials with high conductivity and dispersibility in lead-based materials have the potential to improve the output power of batteries. The carbon material on the negative and positive electrodes forms an asymmetric capacitor with a double-layer capacitance, reducing damage to the battery during high rate or pulse charge/discharge [13]. As a result, LCESBs are suitable for large-scale energy storage due to their safety, low cost, and facile regeneration [14].

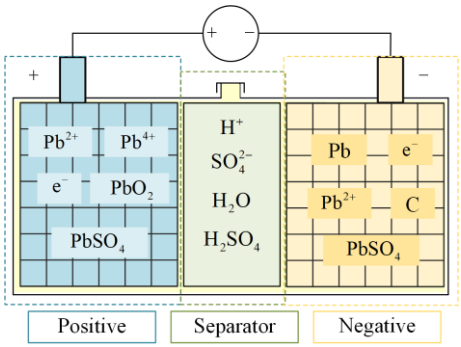

Fig. 1. Schematic diagram of the functioning of LCESBs.

Analyze the three parameters of voltage, resistance, and temperature, and describe their feasibility as characterization parameters.

A. Consistency Analysis of Battery Voltage

The voltage of LCESBs is determined by the difference in electrode potentials of the positive and negative electrode separated by the electrolyte, independently of the shape and size of the batteries. In LCESBs, the open circuit voltage of a single-cell battery is generally about 2.0 V. Meanwhile, the open circuit voltage value is very close to the electromotive force. However, the physical meaning of the latter is clearer, the battery electromotive force can be approximated to the battery voltage. Depending on the actual usage needs, six individual cells can be connected in series to form a single LCESB, with a rated voltage of 12 V.

The electromotive force of LCESBs can be quantitatively described by the Nernst equation [15]:

$$E = -\frac{\Delta G^0}{nF} + \frac{RT}{F}\ln\frac{a(\mathrm{H_2SO_4})}{a(\mathrm{H_2O})} \tag{1}$$

where ΔG^0 represents the difference between the battery reaction product and the standard free energy generated by the reactant; n is the number of electrons; F refers to the Faraday's constant (F=9.65×10000 C/mol); R is the gas constant (R=8.314 J/(mol·K)); T denotes the thermodynamic temperature (K); $a(\mathrm{H_2SO_4})$ presents the activity of $\mathrm{H_2SO_4}$; and $a(\mathrm{H_2O})$ is the activity of $\mathrm{H_2O}$.

The Nernst equation suggests that the battery electromotive force is closely related to the battery material, temperature, and electrolyte concentration. The change in battery voltage during the charge/discharge processes is also related to the current intensity, SOC state, and the amounts of impurities and additives in the electrode. Accordingly, the difference in the electrolyte concentration and SOC state of the battery can result in inconsistent battery voltage.

B. Consistency Analysis of Battery Temperature

The temperature of LCESBs can be determined by the heat of the reversible reaction and joule heat generated by the ohmic resistance. During the electrochemical reaction, the flow of current through the battery results in an equilibrium. In this case, the heat of reversible reaction should only be related to the composition of reactants and their energy states. Under a flow of current, the reversible reaction heat, Q, can be expressed by:

$$Q = I(V - U + T\frac{\partial U}{\partial T}) \tag{2}$$

where I represents the current flowing through the battery; V is the current voltage of the battery; and U refers to the open circuit voltage of the battery.

The Joule heat, Q, generated by the ohmic resistance of a battery under a flow of current can be calculated by:

$$Q = I^2 R_0 t \tag{3}$$

where R_0 represents the battery ohmic resistance; and t is the time duration.

Equations (2) and (3) reveal the temperature changes of the battery, arising due to heat release and absorption by the battery. Based on the thermal process of a reversible reaction, the temperature of the battery would drop as the LCESBs discharges under small currents with an energy quantity below $0.05C$, where C represents the charging or discharging rate.

The temperature of batteries can also be influenced by other factors, such as the magnitude of the current and the duration of charging and discharging. In energy storage battery clusters, the temperature inconsistency between individual battery can influence the accuracy of SOC estimation of the entire cluster. Additionally, this can weaken the discharge power of the entire battery cluster and increase the energy loss, thereby affecting the operational performance of the grid power system.

C. Consistency Analysis of Battery Resistance

The resistance of LCESBs involves ohmic and polarization internal resistances. In turn, the ohmic internal resistance consists of contact and diaphragm resistances. Contact resistance involves metal or alloy resistance and compound resistance, among other components. The diaphragm resistance is related to several parameters, including the material and thickness of the diaphragm, electrolyte concentration, and battery height. Among these, the diaphragm resistance is usually the main factor leading to battery inconsistency.

The resistance of a single battery can be influenced by multiple factors, such as the material, manufacturing process, and operating environment. In series battery clusters, the inconsistency in resistance for single batteries, with the same current, can manifest as a difference in heat generation and voltage change rates of the battery. Inconsistent internal resistance in parallel battery clusters can result in inconsistent charge/discharge levels, depths, and times of individual battery, further affecting the charge/discharge processes of battery clusters.

III. Preliminary Screening of Inconsistent Batteries by High-dimensional Random Matrix Theory

After determining the characterization parameters, high-dimensional random matrix theory is used for preliminary detection of LCESBs. First, parameters like battery voltage, temperature, and resistance of the battery cluster are extracted. The random matrix can then be constructed through the sliding time window. Then, the eigenvalues of each matrix are calculated, and finally the battery voltage consistency is detected by the single loop theorem and average spectral radius. During the preliminary testing, if one of the three characterization parameters is identified through the random matrix as an inconsistent battery, the single battery is considered an inconsistent battery.

A. High-dimensional Random Matrix Theory

In the late 1950s, Wigner elaborated on the study of a large number of particle energy levels in quantum mechanics based on the empirical distribution of the random matrix theory (RMT). Subsequently, mathematicians improved the study of RMT using the knowledge of limit spectrum analysis. Since then, RMT has formed an active branch in modern probability theory. RMT is based on matrices and can handle independently identically distributed data. In addition, RMT does not require the distribution or characteristics of the source data, but only requires the data to be sufficiently large (not infinite). Therefore, this tool is suitable for analyzing massive data systems with a certain degree of randomness [16], [17]. The data dimension for consistency detection of energy storage batteries is generally several hundred dimensions, so using high-dimensional random matrices for consistency detection of energy storage batteries is more advantageous.

The RMT suggests that when there is only white noise, small perturbations, and measurement errors in the system, the data will exhibit a statistical randomness characteristic. When there is a signal source in the system, its operating and internal mechanisms can change under its influence, disrupting its statistical randomness.

Using a random matrix machine for consistency detection of LCESBs requires the construction of a random matrix based on the characterization quantity of the consistency parameter and the average value of the characterization quantity of the cluster of batteries. This can be expressed by:

$$\boldsymbol{X}=\begin{bmatrix} x_t & x_{t+1} & \cdots & x_{t+N-1} \\ x_{\mathrm{ave},t} & x_{\mathrm{ave},t+1} & \cdots & x_{\mathrm{ave},t+N-1} \end{bmatrix} \tag{4}$$

where x_t is the time series of the consistency parameter representation quantity; $x_{\mathrm{ave},t}$ is the time series of the average value of the battery pack representation quantity; and the $\boldsymbol{X}$-matrix row-column ratio is equal to $2/N$, making it difficult to meet the requirements of hundreds or thousands of dimensional data of random matrices. Thus, most studies in literature used translation and block forms to obtain a better row-column ratio. However, this can only suit processing long-term windows and massive data. Additionally, translation and chunking cannot deal with problems of short time windows and small data volumes in battery consistency detection. Alternatively, the sliding window method has been introduced to construct random matrices.

In this work, a sliding window is used to generate a matrix meeting the requirements of random matrix row and column ratio. The sliding window, W, can be defined by:

$$W(m,l,\delta)=\left\{i(t),1+m\delta\leqslant t\leqslant l+m\delta\right\},m=1,2,\cdots,M \tag{5}$$

where m is the number of times the window slides; l represents the length of the sliding window; and δ is the sliding factor taken as 1 to express sliding back one point each time.

The final construction matrix can be written as follows:

$$\boldsymbol{X}=\begin{bmatrix} x_t & x_{t+1} & \cdots & x_{t+N-1} \\ x_{\mathrm{ave},t} & x_{\mathrm{ave},t+1} & \cdots & x_{\mathrm{ave},t+N-1} \\ \vdots & \vdots & & \vdots \\ x_{t+M/2-1} & x_{t+M/2} & \cdots & x_{t+M/2+N-2} \\ x_{\mathrm{ave},t+M/2-1} & x_{\mathrm{ave},t+M/2} & \cdots & x_{\mathrm{ave},t+M/2+N-2} \end{bmatrix} \tag{6}$$

where $x_{t+M/2-1}$ is the characterization quantity of the consistency parameter at time $t+M/2-1$; $x_{\mathrm{ave},t+M/2-1}$ is the average value of the characterization quantity of the cluster of batteries at time $t+M/2-1$.

B. Single Ring Theorem

The single loop theorem is a significant breakthrough in the RMT system, which can be used to study the linear eigenvalue statistics (LES) of random matrices. From a macro perspective, the distribution trend of system eigenvalues can be analyzed using the single loop theorem. Combining the inner and outer loop radii to analyze the statistical characteristics of eigenvalues distribution can help qualitatively evaluate the system state. When applying the RMT to consistency detection, batteries with consistent characteristics exhibit randomness in their data. In the single loop theorem, battery with consistent characteristics is manifested as the distribution of eigenvalues in the outer loop. If there are inconsistent batteries, their randomness generally breaks the single loop theorem, and the matrix eigenvalues will be distributed in the inner loop.

For data matrix $\boldsymbol{X}=\{x_{i,j}\}_{M\times N}$ with non-Hermitian features of M rows and N columns, the matrix expectation $E(x_{i,j})=0$ should satisfy the matrix variance $E(|x_{i,j}|^2)=1$. The non-Hermitian matrix $\boldsymbol{X}_i(i=1,2,\cdots,L)$, corre-

sponding to the product matrix of the singular-valued equivalence matrix $\boldsymbol{Z}=\prod_{i=1}^{L}\boldsymbol{X}_{u,i}$, can normalize the $\boldsymbol{Z}$ matrix to yield the standard matrix product $\tilde{\boldsymbol{Z}}$ shown as follows:

$$\tilde{z}_i = z_i \Big/ \left[\sqrt{M}\sigma(z_i)\right],\ i=1,2,\cdots,M \tag{7}$$

where $\sigma(z_i)$ is the standard deviation of $\boldsymbol{X}$. When the row-column ratio $c=M/N\in(0,1]$ and M, N approach infinity, the empirical spectral distribution of $\tilde{\boldsymbol{Z}}$ eigenvalue λ_i converges to the given limit. In this case, the probability density function $f_{\tilde{Z}}(\lambda)$ can be given as follows:

$$f_{\tilde{Z}}(\lambda)=\begin{cases}\dfrac{2}{\pi cL}|\lambda|^{(2/L-1)}, (1-c)^{L/2}\leqslant|\lambda|\leqslant 1\\ 0,\ \text{others}\end{cases} \tag{8}$$

where λ represents the eigenvalue; and L is the number of Hermitian matrices.

For the single ring theorem, the standard non-Hermitian matrix $\boldsymbol{X}$, with each element taken as an independent homogeneous Gaussian random variable, can be roughly distributed in a ring, with an outer diameter of r_1=1 and inner diameter of r_2=$(1-c)^{L/2}$, presented in the complex plane.

Consistent battery factors, such as voltage, resistance, and temperature, with the average value of the battery would result in independent elements in the matrix. This would lead to a uniform distribution of all the matrix eigenvalues in the outer ring, as shown in Fig. 2(a). On the other hand, the inconsistent battery factors, such as voltage, resistance, and temperature deviating from their average values, can lead to a matrix that no longer obeys the independent and identically distributed principles. Additionally, all the matrix eigenvalues should be distributed in the inner ring, as shown in Fig. 2(b).

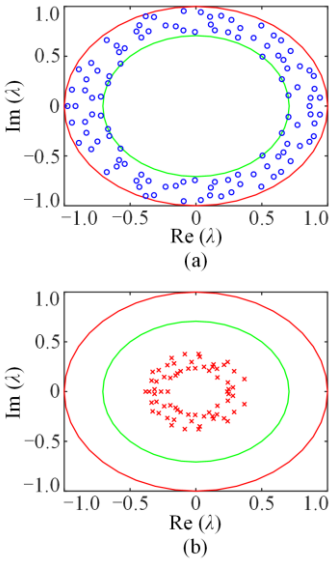

Fig. 2. Monocyclic theorem of the random matrix eigenvalues distributed in the outer ring. (a) Outer ring. (b) Inner ring.

C. Linear Eigenroot Statistic

The LES can be used to reflect the distribution of the eigenvalues of a random matrix, with a commonly used type of random matrix theory consisting of mean spectral radius (MSR). Here, combined with the single-ring theorem, the spectral radius is employed to reflect the distribution of the eigenvalues. The spectral radius for a matrix product $\tilde{\boldsymbol{Z}}$ can be defined as follows:

$$r_{\text{MSR}}=\frac{1}{N}\sum_{i=1}^{N}\left|\lambda_{\tilde{Z},i}\right| \tag{9}$$

where $\lambda_{\tilde{Z},i}$ represents the ith eigenvalue of the matrix product. For the random matrix, a single eigenvalue can not reflect the statistical characteristics of the matrix elements. The LES may describe the trace of the random matrix, while the trace can reflect the statistical characteristics of the matrix. Consequently, the average spectral radius can be used as a criterion index.

IV. Accurate Detection of Distance Consistency Based on SOD Combined with Wasserstein

After the preliminary consistency testing, to accurately detect the voltage consistency of battery clusters, the test data is first be subjected to the SOD transformation to extract the voltage variation features. The Wasserstein distance is then used to calculate the distance between the voltage feature distribution of the ith battery and the average voltage feature distribution of the battery cluster. The consistency of the ith battery may be judged based on the Wasserstein distance. The precise detection of temperature consistency should be consistent with the precise detection method of voltage consistency.

A. SOD Transform

SOD, a high-order differential operation, is essentially a high-order differential. The higher the differential order, the more accurate are the results obtained, which can reflect the characteristics and mutation direction of high-frequency transient signals [18], [19]. When SOD is applied for the precise detection of energy storage consistency, the differences in voltage, temperature, and resistance of inconsistent batteries are amplified, thereby more accurately screening inconsistent batteries. This can be described by:

$$S_k(n)=\sum_{j=1}^{k+1}(-1)^{j+1}(c_j)_k Q(n-j+1) \tag{10}$$

where k represents the order of the difference; j represents the jth SOD transformation; $S_k(n)$ is the k-order differential of the signal; Q refers to the original signal; n is the number of instantaneous sampling points starting at least from (k+1); and $(c_j)_k$ denotes the SOD transformation coef ficient calculated by (11)–(14).

1) The first and last coefficients of the SOD transformation are equal and are equal to 1, as shown by:

$$(c_1)_k = (c_{k+1})_k = 1 \tag{11}$$

2) The second coefficient of the SOD transformation is the order of the SOD transformation as depicted by:

$$(c_2)_k = k \tag{12}$$

3) Other coefficients of the SOD transformation can be calculated by:

$$(c_j)_k = (c_j)_{k-1} + (c_{j-1})_k \tag{13}$$

Here, the sum of all SOD coefficients is 0, shown as:

$$\sum (-1)^{j+1} (c_j)_k = 0 \tag{14}$$

In (10), n starts from (k+1), and every (k+1)th sample point is calculated. The number obtained by the first (k+1)th sample point operation is then used as the first number of a new set. Then, the previous operation is repeated by one sample point, and a new set of data are obtained after transformation, forming a k-order SOD transformation signal.

After deduction, the 4th-order and 5th-order SOD transformations are respectively shown by:

$$S_4(n) = Q(n) - 4Q(n-1) + 6Q(n-2) - 4Q(n-3) + Q(n-4) \tag{15}$$

$$S_5(n) = Q(n) - 5Q(n-1) + 10Q(n-2) - 10Q(n-3) + 5Q(n-4) - Q(n-5) \tag{16}$$

where $Q(n)$ refers to the original signal.

For accurate detection of the consistency of LCESBs, it is necessary to determine the order η when extracting features, U_s and T_s, from the measured voltage and temperature sampling data of LCESBs through the SOD transformation.

B. Wasserstein Distance

The Wasserstein distance can be used to evaluate the similarity and continuity of the two distributions. The latter can support sets of the two distributions with less or no overlapping, while still reflecting the similarity of the two distributions [20], [21]. The characteristic distribution of consistent batteries is often denoted by the P_1 distribution, while the current characteristic distribution of the batteries is referred to as the P_2 distribution. The consistency of the current battery can be determined by extracting the difference between the P_1 and P_2 distributions through the Wasserstein distance. The Wasserstein distance application in the battery consistency detection has several unique advantages. First, sets of two distributions, with less or no overlapping, can still reflect the distance between the two distributions, thereby determining the battery consistency state. Second, the distance with continuity should induce characteristics of SOD transformation with continuity. The Wasserstein distance can be expressed according to:

$$W(P_1, P_2) = \inf_{\gamma \sim \Pi(P_1, P_2)} \mathbb{E}_{(x,y)\sim\gamma} \left[\|x - y\| \right] \tag{17}$$

where $\Pi(P_1,P_2)$ represents the set of all possible joint distributions combining the P_1 and P_2 distributions; for each possible joint distribution γ, samples x and y can be obtained by sampling $(x, y) \sim \gamma$, and the distance $\|x - y\|$ between these samples can be calculated. Therefore, the expected distance of the samples under this joint distribution, γ, can be calculated. The Wasserstein distance refers to the lower bound $\inf_{\gamma \sim \Pi(P_1, P_2)} \mathbb{E}_{(x,y)\sim\gamma} \left[\|x - y\| \right]$ for the expected value in all possible joint distributions.

V. Evaluation of Consistency Detection Algorithm Reliability

A confusion matrix is used to evaluate the reliability of accurate detection results. The confusion matrix, as a visual tool for the accurate performance of classification algorithms, can be employed for the accuracy evaluation of battery consistency detection due to no constraint by the amount of data [22], [23]. The form of the confusion matrix, $\boldsymbol{Q}$, is summarized in Fig. 3.

Confusion matrix		Forecast class	
		Consistency (1)	Inconsistency (0)
Actual class	Consistency (1)	True consistency (TC)	False consistency (FC)
	Inconsistency (0)	False inconsistency (FI)	True inconsistency (TI)

Fig. 3. Confusion matrix principle.

Since matrix $\boldsymbol{Q}$ is a second-order square matrix, the consistent battery in this work is marked as 1, while the inconsistent battery is marked as 0. For the reference classification of 1 and prediction classification of 1, the true consistency value (v_{TC}) will be added by 1. For the reference classification of 1 and predicted classification of 0, the false consistency value (v_{FC}) will increase by 1. For reference classification of 0 and prediction classification of 1, the false inconsistency value (v_{FI}) will increase by 1. Finally, for the reference classification of 0 and predicted classification of 0, the true inconsistency value (v_{TI}) will increase by 1.

A false negative rate of the confusion matrix for inconsistent batteries is detected as consistent battery, δ, which can be expressed by:

$$\delta = \frac{v_{FI}}{v_{FI} + v_{TC}} \times 100\% \tag{18}$$

The results obtained from the detection algorithm with the actual battery are compared using accuracy μ, calculated by:

$$\mu = \frac{v_{TC} + v_{TI}}{v_{TC} + v_{TI} + v_{FC} + v_{FI}} \times 100\% \tag{19}$$

False negative rates δ obtained through the confusion matrix, and accuracy μ, can be employed to quantify the

reliability of the proposed algorithm. For the battery consistency detection algorithm, a false negative rate indicates that the algorithm has missed detection and should not be used.

The consistency detection flow chart is provided in Fig. 4. In this case, the random matrix is first used for the initial consistency detection. For batteries inconsistent in the initial detection, the SOD and Wasserstein distance are utilized for the second accurate detection. Finally, the reliability of the algorithm is evaluated.

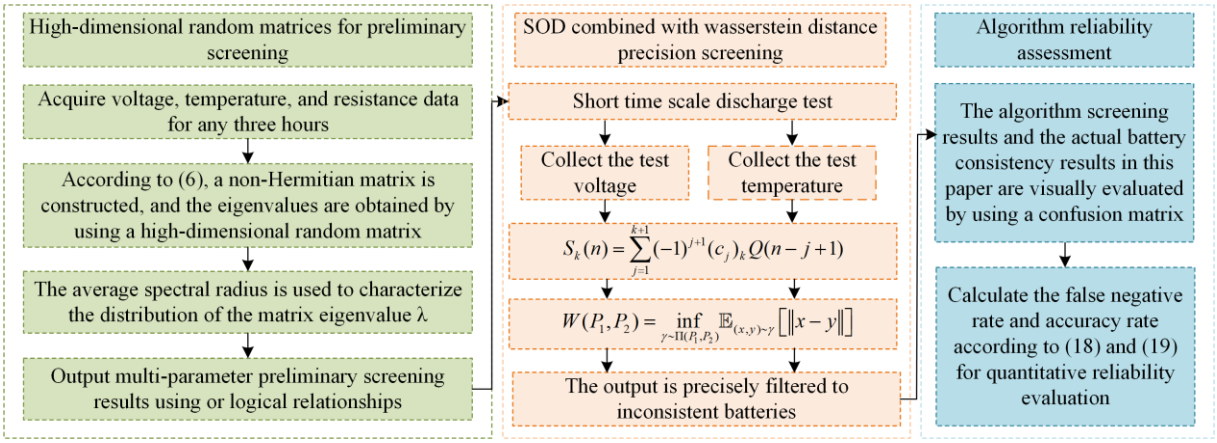

Fig. 4. Consistency detection flowchart.

VI. Verification of the Measured Data

In this case study, the 0.5 MW/2 MWh LCESBs system configured in the photovoltaic, energy storage, and charging pile (integrated construction project of Kunming Hendera Science and Technology Co., Ltd.) is used. 1680 LCESBs are studied, and the battery parameters are 12 V and 100 Ah, with clusters containing 40 batteries each, totaling 42 clusters. To verify the accuracy of the method proposed in this article, the inconsistent batteries are replaced with the original batteries for testing. The inconsistent battery numbers are (1, 28), (3, 22), (5, 38), (9, 39), (11, 18), (25, 17), (35, 22), and (42, 39).

Taking the first cluster of batteries as an example, preliminary consistency checks are conducted on the voltage, temperature, and resistance values. The first cluster of the LCESBs and BMS are shown in Fig. 5.

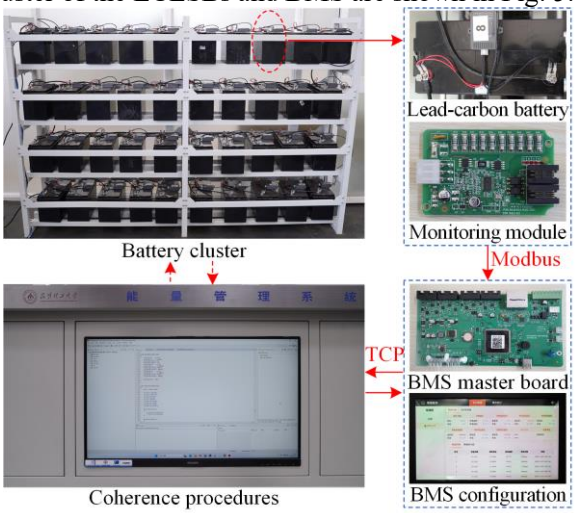

Fig. 5. Consistency testing platform for LCESBs.

The batteries are equipped with detection modules for monitoring the battery voltage, temperature, and internal resistance. The monitoring modules transmitted signals to the BMS main control board and BMS configuration through the Modbus protocol, and consequently to the energy management system (EMS), through the transmission control protocol (TCP) protocol. The consistency detection algorithm proposed in this study is embedded in the BMS for monitoring inconsistent batteries.

A. Preliminary Consistency Detection Based on Random Matrix

The voltage, temperature, and resistance of the first cluster of LCESBs collected by the BMS are preliminarily checked for consistency using a random matrix.

1) Preliminary Detection Based on Voltage

The voltage data of the LCESBs standing for 3 hour are collected and the results are shown in Fig. 6.

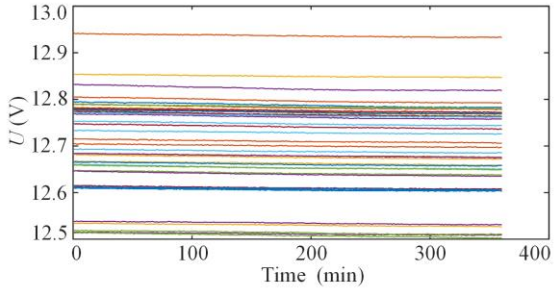

Fig. 6. Voltage data curve of LCESBs at a standstill.

Under stationary conditions, the voltage of LCESBs ranged from 12.5 V to 12.8 V, with some batteries reaching a significantly higher voltage of 12.95 V. The average value of the cluster of batteries is then obtained by removing the maximum and minimum values. A random matrix $\boldsymbol{X}_{M\times N}$ based on (6) is constructed for the voltage of a single battery and the average voltage of the cluster of batteries. Next, the distribution of characteristic values for each battery in the cluster is calculated, as summarized in Fig. 7.

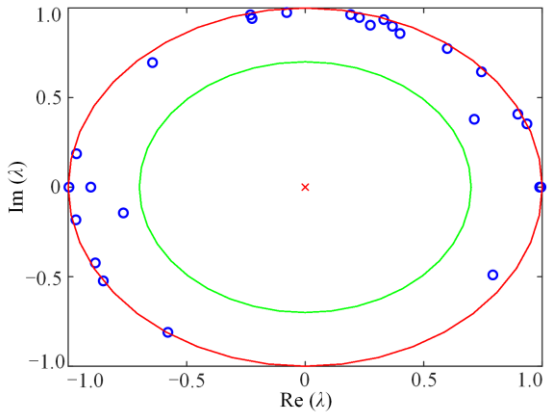

Fig. 7. Average spectral radius distribution of battery cluster voltage.

Since the average spectral radius of only one battery in the cluster is distributed in the inner ring, the number of inconsistent batteries in the cluster determined by the voltage characterization quantity is 1.

2) Preliminary Detection Based on Temperature

The temperature data of the batteries standing for 3 hours are collected and analyzed, as shown in Fig. 8.

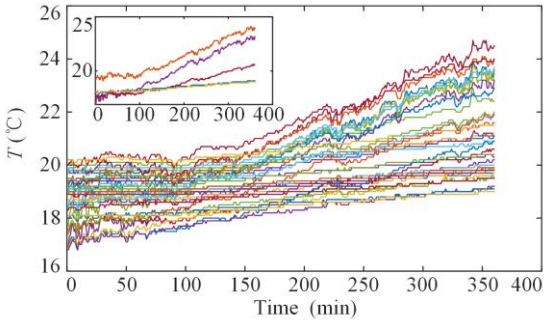

Fig. 8. Temperature curves of LCESBs.

The temperature of a battery remained within a certain range without significant deviation. However, different batteries exhibited different changing rates as a function of temperature. Thus, the eigenvalues of each battery in the cluster are calculated, and the average spectral radius is employed to reflect the distribution of the eigenvalues of each battery in the cluster as shown in Fig. 9.

In Fig. 9, the average spectral radius of two batteries is distributed in the inner ring. According to the temperature characterization quantity, the number of inconsistent batteries in this cluster is 2.

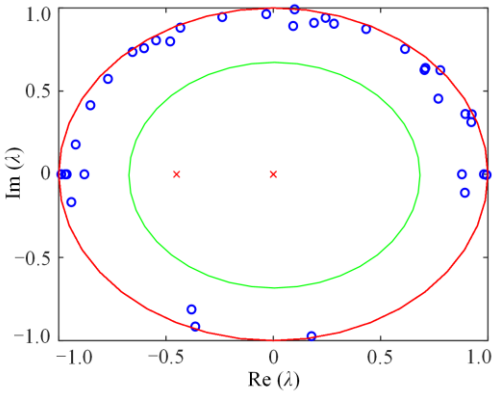

Fig. 9. Average spectral radius distribution of the battery cluster temperature.

3) Preliminary Detection Based on Resistance

The resistance data of the batteries standing for 3 hour are collected, as shown in Fig. 10.

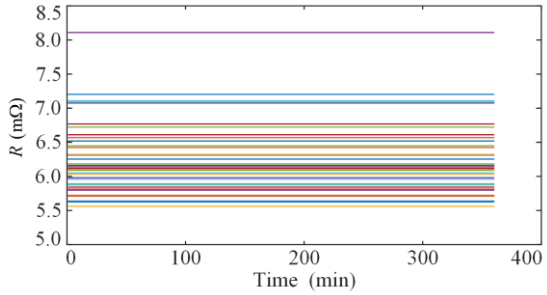

Fig. 10. Resistance curve of LCESBs when standing still.

Figure 10 shows a battery with a resistance exceeding 8 mΩ, significantly deviating from the typical value of 6 mΩ recorded for most batteries. Hence, the eigenvalues of each battery in the cluster are calculated, and the average spectral radius is used to reflect the distribution of the eigenvalues of each battery in the cluster as shown in Fig. 11.

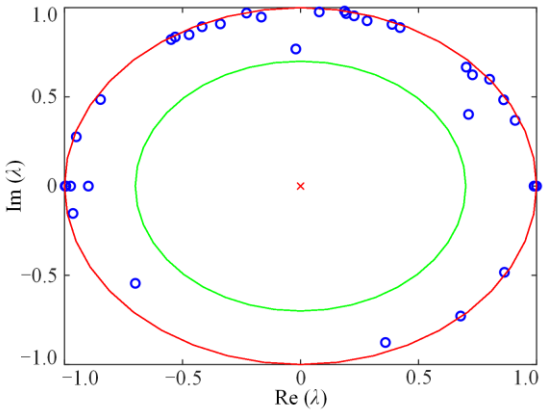

Fig. 11. Average spectral radius distribution of battery cluster resistance.

The average spectral radius of one cell fell on the inner ring, while other cells showed distributions on the outer ring. Therefore, the number of inconsistent cells in this cluster is 1, which is consistent with the resistance value of one cell in Fig. 11, and is significantly different from most other cells.

Three characterization parameters (voltage, temperature, and resistance) are used to determine the inconsistent batteries in the cluster during the preliminary detection process through the logical OR. The preliminary detection revealed (1, 18) and (1, 28) as inconsistent batteries in the cluster.

The remaining battery clusters are identified using the same preliminary detection method, and the results are summarized in Table I. A total of 28 batteries are preliminarily determined as inconsistent, thereby requiring precise detection.

TABLE I
INITIAL DETECTION OF INCONSISTENT BATTERIES

Battery cluster	Inconsistent battery serial number	Battery cluster	Inconsistent battery serial number
1	18,28	22	No
2	No	23	No
3	22	24	28
4	19	25	17
5	38	26	No
6	No	27	27
7	12	28	No
8	22	29	35
9	39	30	29
10	No	31	36
11	18	32	30
12	12,16	33	No
13	No	34	21
14	25	35	22
15	36	36	No
16	18	37	No
17	No	38	18
18	No	39	No
19	No	40	34
20	24	41	No
21	3	42	39

B. Accurate Detection of Consistency

The 28 batteries initially determined as inconsistent are numbered 1–28. A short-term discharge test is conducted for 10 min, with a discharge rate of 1*C*. The data is collected for a total of 20 min, including 5 min before, 10 min during, and 5 min after testing.

1) Accurate Detection Based on the Test Voltage

The consistency of the battery voltage is determined according to the Chinese standard "GB/T 36280-2018 Lead Carbon Batteries for Electric Energy Storage." Since the difference in the terminal voltage between the 12 V batteries during the battery cluster operation should not exceed 600 mV, a voltage of ±0.3V (300 mV) is taken as the critical point, and transformed from the mean voltage through the 4th-order SOD. The Wasserstein distance is calculated as 0.31, and set as the threshold. The Wasserstein distance of an individual battery voltage above the threshold resulted in voltage inconsistency of the battery; otherwise, a consistency battery is identified.

The test voltage data of 28 batteries with inconsistent initial detection are presented in Fig. 12.

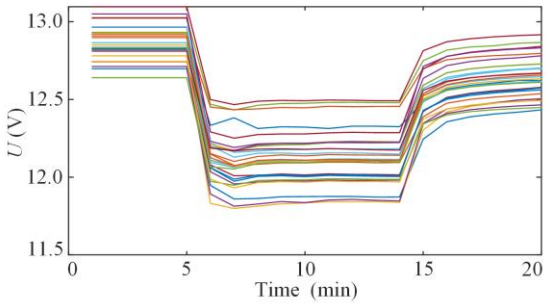

Fig. 12. Discharge test voltage curves of 28 batteries.

In Fig. 12, a total of three curves deviate below, while five curves deviate above.

A certain test voltage curve of an LCESB is provided in Fig. 13(a). During testing, the voltage change value remains at about 0.96 V. The voltage data of the LCESB is then transformed into a 2nd–5th order SOD to obtain Fig. 13(b). The amplitude of the 2nd and 3rd orders of the SOD transformation are both about 1.5 V. Additionally, the amplitude of the 4th-order SOD transformation is more than 2-fold the original difference, and that of the 5th-order SOD transformation is more than 3-fold the original difference. The difference in amplitude between the 4th-order SOD transformation and the 5th-order SOD transformation of LCESB both exceed the two-fold. However, since the computational complexity of the 4th-order SOD transformation is smaller than that of the fifth-order SOD transformation, the 4th-order SOD transformation is chosen.

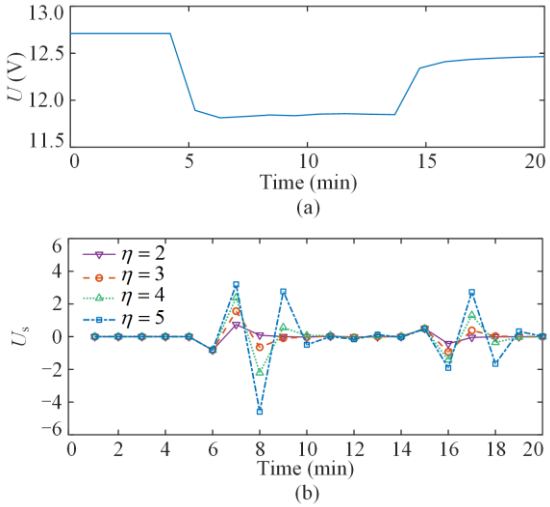

Fig. 13. Test voltage and SOD conversion curves. (a) Measured voltage curve. (b) SOD transform eigenvalue curve.

The 4th-order SOD changes in the test voltage data are used to extract the transformation features as shown in Fig. 14.

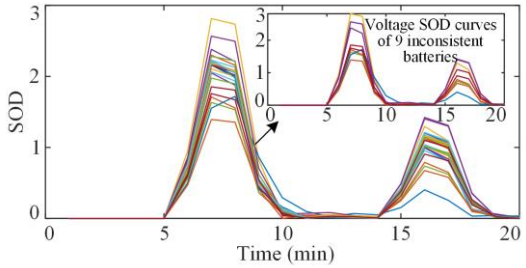

Fig. 14. Profiles of test voltage 4th-order SOD continuous characteristics.

The Wasserstein distance of the *i*th battery voltage is calculated along with the voltage means after the 4th-order SOD transformation, as shown in Fig. 15.

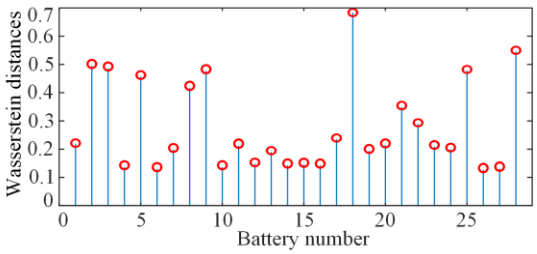

Fig. 15. Voltage SOD transformation feature Wasserstein distance.

The Wasserstein distances of batteries 2, 3, 5, 8, 9, 18, 21, 25, and 28 are estimated to be 0.497, 0.494, 0.472, 0.412, 0.481, 0.693, 0.348, 0.486, and 0.547, respectively. Batteries exceeding the threshold are considered inconsistent and the original numbers are identified as (1, 28), (3, 22), (5, 38), (9, 39), (11, 18), (25, 17), (30, 29), (35, 22), and (42, 39).

2) Accurate Detection Based on the Test Temperature

Reference [24] models the battery clusters and suggests a possible control of the temperature difference within the battery cluster at 10°C, without considering the cycle life of the battery cluster. Reference [25] proposes a temperature difference between individual cells not exceeding 5°C to ensure consistent individual cells in the battery cluster. Accordingly, ±2.5°C is taken as the critical point to transform, with the temperature mean, through a 5th-order SOD. The Wasserstein distance is calculated as 1.98 and set as the threshold. The Wasserstein distance of the battery temperature is greater than the threshold resulted in voltage inconsistency in the batteries; otherwise, the batteries are consistent.

The collected temperature data for short-term discharge testing of the 28 batteries are provided in Fig. 16. Batteries undergoing a high-rate discharge result in an increase in the battery temperature in a short period.

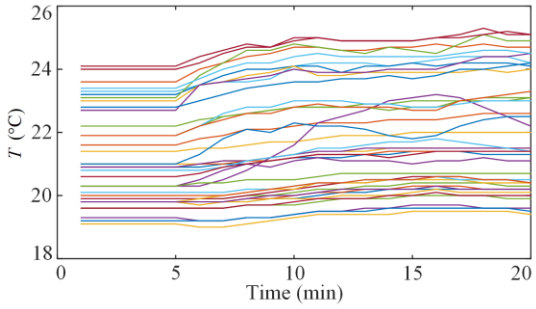

Fig. 16. Discharge test temperature curve of 28 batteries.

A certain test temperature curve of an LCESB is provided in Fig. 17(a). A temperature change value of about 3°C is recorded during the testing process. The resulting temperature data of the LCESBs are then transformed into a 2nd–5th order SOD to yield Fig. 17(b). The transformation characteristics and amplitude appeared different under the 2nd-order, 3rd-order, and 4th-order SOD transformations. Meanwhile, the transformation characteristics appear more obvious using the 5th-order SOD transformation. According to the SOD transformation theory and analysis shown in Fig. 17(b), the difference in the characteristics of the 5th-order SOD transformation appear more significant. Thus, the 5th-order SOD transformation is selected for subsequent study and analysis.

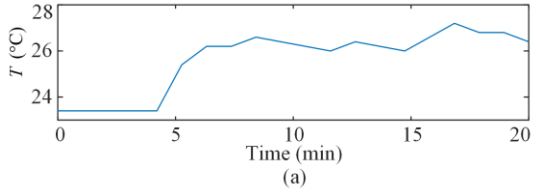

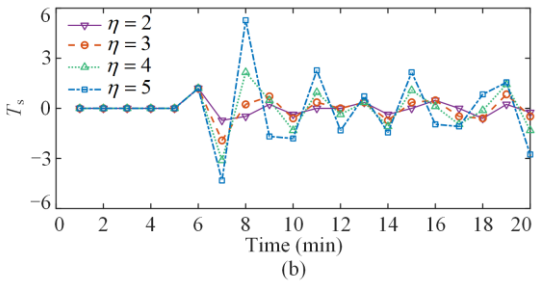

Fig. 17. Test temperature and SOD conversion curves. (a) Measured temperature profile. (b) SOD transform eigenvalue curve.

The extracted features from the 5th-order SOD changes of the test temperature data are displayed in Fig. 18.

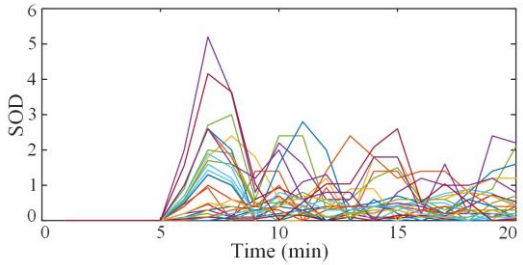

Fig. 18. Continuous characteristics of the 5th-order SOD at the test temperature.

The Wasserstein distances for calculating the temperature and mean temperature of the *i*th battery, after the 5th-order SOD transformation, are shown in Fig. 19.

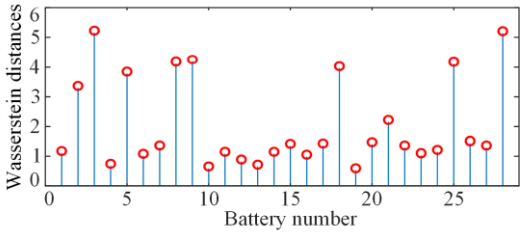

Fig. 19. Wasserstein distance of the temperature SOD transformation feature.

The results obtained based on temperature appear similar to those obtained based on voltage. Inconsistent batteries are identified to be (1, 28), (3, 22), (5, 38), (9, 39), (11, 18), (25, 17), (30, 29), (35, 22), and (42, 39).

A total of 28 batteries are accurately tested for multiple parameters. The results indicate that during the initial testing process, 9 batteries are inconsistent, while 19 are mistakenly detected as inconsistent.

The confusion matrix is used to qualitatively and quantitatively analyze the false negative rate of the algorithm, δ, and accuracy, μ, as shown in Fig. 20.

Confusion matrix		Forecast class	
		Consistency (1)	Inconsistency (0)
Actual class	Consistency (1)	1671	1
	Inconsistency (0)	0	8

Fig. 20. False negative rate and accuracy of the algorithm in this study.

The false negative rate of the algorithm, δ, can be expressed by:

$$\delta = \frac{0}{0+1671} \times 100\% = 0\% \tag{20}$$

The accuracy of the algorithm, μ, is calculated by:

$$\mu = \frac{1671+8}{1680} \times 100\% = 99.94\% \tag{21}$$

The negative rate of the algorithm, δ, is quantitatively calculated as 0. Thus, the algorithm does not detect the actual inconsistent batteries as consistent ones, with an accuracy rate, μ, determined as 99.94%.

C. Comparative Analysis of Test Results

The accuracy of the proposed algorithm is compared to those of the PCA, K-means, and FCM clustering methods.

The consistency testing of the LCESBs is then carried out by the three algorithms mentioned above using the voltage, temperature, and resistance data in Section VI.A. The results are shown in Figs. 21–23.

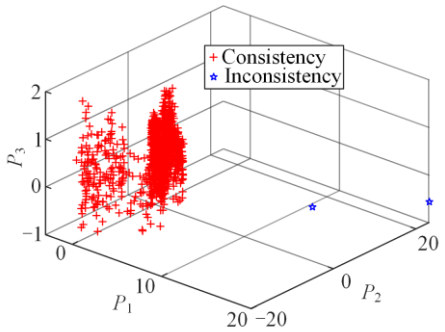

Fig. 21. Consistency detection based on principal component analysis.

Using the principal component analysis algorithm, the dimensionality of high-dimensional data is reduced to principal components 1, 2, and 3, in three dimensions. By detecting the battery consistency through 3D (D is the dimension) data, only 2 batteries are detected as inconsistent, and 6 batteries are not detected as inconsistent.

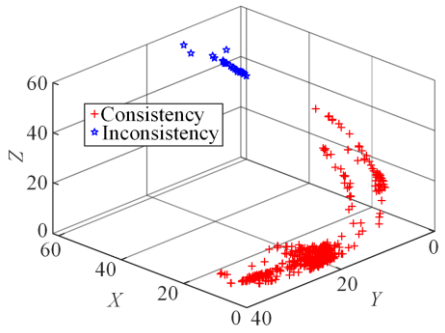

Fig. 22. Consistency detection based on K-means.

The voltage, temperature, and resistance are normalized as inputs for clustering utilizing the K-means clustering algorithm. To this end, the first, second, and third eigenvalues are represented by X, Y, and Z, respectively. Results indicate 30 inconsistent batteries. This algorithm mistakenly detect 22 consistent batteries as inconsistent batteries.

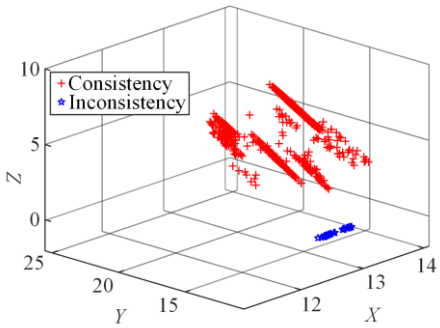

Fig. 23. Consistency detection based on FCM.

Furthermore, 52 batteries are clustered into inconsistent batteries using the FCM clustering algorithm. While this algorithm does not miss the detection of inconsistent batteries, it mistakenly detect 44 consistent batteries as inconsistent.

The false negative rates of the above three algorithms are then calculated by (18) and (19). The values of δ and μ are shown in Table II.

TABLE II
ALGORITHM FALSE NEGATIVE RATE AND ACCURACY CALCULATION

Detection algorithms	False negative rate (%)	Accuracy (%)
The proposed algorithm	0	99.94
PCA	0.32	99.64
K-means	0	98.69
FCM	0	97.38

The false negative rate of PCA in Table II is 0.32%, with an accuracy rate of 99.64%. The false negative rate of the K-means clustering is 0, and the accuracy rate is 98.69%. The false negative rate of the FCM clustering is 0, and the accuracy rate is 97.38%. While the accuracy of the PCA algorithm is relatively high, the false negative rate of the algorithm is not zero. Even if the algorithm is used for detection, there may still be inconsistent batteries, which can affect the performance and service life of the battery cluster. The K-means and FCM clustering algorithms have slightly lower accuracy, which may increase the operation and maintenance costs of the LCESBs. The false negative rate of the algorithm used in this article is 0, and the accuracy rate is 99.94%, demonstrating a high accuracy without missing detections. Compared to the PCA, K-means, and FCM clustering methods, the proposed random matrix preliminary screening and SOD precise screening methods are suitable for consistency detection in large-scale energy storage systems.

VII. CONCLUSION

To solve the problem of inconsistency in the use of LCESBs and the difficulty of large-scale consistency detection, a method based on random matrix theory for preliminary detection and precise SOD detection is proposed. The conclusions of this study are summarized as follows.

1) Typical energy storage stations have a large number of batteries, resulting in a significant amount of voltage, temperature, and resistance data. Random matrices have advantages in handling high-dimensional data. The single loop theorem and average spectral radius can be used for quantitative analysis and to visually present the results of random matrix calculations for battery consistency, enabling preliminary testing.

2) SOD is used to amplify the characteristic voltage and temperature changes of LCESBs. Then, the Wasserstein distance of voltage and temperature, after the SOD transformation, is calculated, to accurately detect battery consistency.

3) A confusion matrix is used to calculate the false negative rate and precision of the consistency detection algorithm. The algorithm is quantitatively and qualitatively evaluated, and its reliability is validated.

4) The accuracy of the proposed algorithm is found to be 99.94%, which is higher than those obtained by PCA, K-means, and FCM. The false negative rate of the proposed algorithm is 0, indicating no missed detections. In contrast, PCA shows non-zero false negative rates, indicating missed detections.

The proposed algorithm helps avoid missed detections, reduce false alarms, and improve the accuracy and reliability of consistency detection. The method can lead to improved the operational performance and service life of large-scale LCESBs. However, the proposed consistency detection method only utilizes three characterization parameters, i.e., voltage, temperature, and resistance. In future research, characterization parameters, such as battery capacity, SOC, and SOH, can also be considered for more comprehensive and accurate detection of the consistency of large-scale LCESBs.

ACKNOWLEDGMENT

Dedicated to the 70th Anniversary of Kunming University of Science and Technology.

AUTHORS' CONTRIBUTIONS

Hongchun Shu: ideas, and formulation of overarching research goals and aims. Guangxue Wang: writing-reviewing, editing, and methodology. Wenlong Li: data curation, and writing-original draft preparation. Botao Shi: supervision, conducting a research and investigation process. Zhongcheng Guo: data collection. All authors read and approved the final manuscript.

FUNDING

This work is supported in part by the National Natural Science Foundation of China (No. 52037003), and the Major Science and Technology Projects in Yunnan Province (No. 202402AG050006).

AVAILABILITY OF DATA AND MATERIALS

Please contact the corresponding author for data material request.

DECLARATIONS

Competing interests: The authors declare that they have no known competing financial interests or personal relationships that could have appeared to influence the work reported in this article.

AUTHORS' INFORMATION

Hongchun Shu received his Ph.D. degree in electrical engineering from the Harbin Institute of Technology, China, in 1997. He became a professor in 1998 and completed his postdoctoral study from the Xi'an Jiao Tong University in 1999. He is currently among the famous teachers in the Yunnan Province, winning the first teaching merit of the Yunnan Province, the title of the national model teachers, the national excellent teachers, the National May 1 Labor Medal and the national excellent science and technology workers award. He presided over a total of 13 projects, including key and general projects of the National Natural Science Foundation of China, "863" projects of the Yunnan province. He has to his credit more than 100 inventions as a first inventor, six books published by the state-level publishing press, 200 EI or SCI indexed papers, and one enterprise standard. He is currently a second-grade professor in China and a supervisor of Ph.D. students. His research interests include active support technologies for renewable energy power systems, fault location of distribution power system, protection and HVDC.

Guangxue Wang received the B.Eng. degree from the University of Jinan, China, in 2017. He is currently a Ph.D. student at the Kunming University of Science and Technology. His research interests include energy storage technology, renewable energy system control and HVDC transmission protection.

Wenlong Li received his B.Eng. degree from the Yunnan Minzu University, China in 2021. He is currently a M.Sc. student at the Kunming University of Science and Technology. His research interest covers new power systems and energy storage.

Botao Shi received his B.Eng. degree from Zhengzhou Technology and Business University in 2021. He is currently pursuing a master's degree in power engineering at Kunming University of Science and Technology. The main research direction for energy storage technology, renewable energy technologies.

Zhongcheng Guo is a professor. In 1998, he was a visiting scholar in the Materials Department of Monash University in Australia, and served as the chairman and general manager of Kunming Hendera Science and Technology Co., Ltd. He hosted and completed more

than 20 projects, including the National 863 Program and the National Natural Science Foundation of China, received the National Excellent Doctoral Dissertation Award from the Ministry of Education of China, and published over 200 core papers, 9 monographs and more than 40 authorized patents. His main research direction is large-scale energy storage technology.

REFERENCES

[1] J. Li, G. Mu, and J. Zhang *et al*., "Dynamic economic evaluation of hundred megawatt-scale electrochemical energy storage for auxiliary peak shaving," *Protection and Control of Modern Power Systems*, vol. 8, no. 3, Jul. 2023.

[2] T. Wang and B. Suo (2023, Mar.), "Low-carbon electricity technology transformation in Chinese universities," *International Journal of Climate Change Strategies and Management*, [Online]. Available: https://doi.org/10.1108/IJCCSM-08-2022-0121

[3] X. Yao, S. Ma, and Y. Fan *et al*., "An investigation of battery storage operating strategies in the context of smart cities," *Industrial Management & Data Systems*, vol. 122, no. 10, pp. 2393-2415, Aug. 2022.

[4] Y. Qin, Z. Xu, and S. Xiao *et al*., "Temperature consistency-oriented rapid heating strategy combining pulsed operation and external thermal management for lithium-ion batteries," *Applied Energy*, vol. 335, no. 120659, Apr. 2023.

[5] X. Fan, W. Zhang, and B. Sun *et al*., "Battery pack consistency modeling based on generative adversarial networks," *Energy*, vol. 239, no. 122419, Jan. 2022.

[6] J. Liu and X. Liu, "An improved method of state of health prediction for lithium batteries considering different temperature," *Journal of Energy Storage*, vol. 63, no. 107028, Jul. 2023.

[7] N. Yan, X. Li, and Y. Zhong *et al*., "Stepwise screening method for retired power battery modules based on static-dynamic consistency," *Proceedings of the CSEE*, vol. 43, no. 5, pp. 2060-2069, Jul. 2023.

[8] M. Cai, S. Wang, and K. Wang *et al*., "A sorting method for series connected liquid metal battery modules," *Proceedings of the CSEE*, vol. 43, no. 14, pp. 5450-5460, Jul. 2023.

[9] H. Wang, K. Yu, and L. Mao *et al*., "Evaluation of lithium-ion battery pack capacity consistency using one-dimensional magnetic field scanning," *IEEE Transactions Instrumentation and Measurement*, vol. 71, no. 3507610, Apr. 2022.

[10] Z. Zhou, A. Ran, and S. Chen *et al*., "A fast screening framework for second-life batteries based on an improved bisecting K-means algorithm combined with fast pulse test," *Journal of Energy Storage*, vol. 31, no. 101739, Oct. 2020.

[11] L. Wang, L. Wang, and C. Liao *et al*., "Research on multi-parameter evaluation of electric vehicle power battery consistency based on principal component analysis," *Journal of Shanghai Jiaotong University (Science)*, vol. 23, no. 5, pp. 711-720, Aug. 2018.

[12] Z. Wang, X. Tuo, and J. Zhou *et al*., "Performance study of large capacity industrial lead-carbon battery for energy storage," *Journal of Energy Storage*, vol. 55, no. 105398, Nov. 2022.

[13] N. Vangapally, T. R. Penki, and Y. Elias *et al*., "Lead-acid batteries and lead-carbon hybrid systems: a review," *Journal of Power Sources*, vol. 579, no. 233312, Sept. 2023.

[14] H. Shu, W. Li, and G. Wang *et al*., "Online collaborative estimation technology for SOC and SOH of frequency regulation of a lead-carbon battery in a power system with a high proportion of renewable energy," *Protection and Control of Modern Power Systems*, vol. 9, no. 1, pp. 52-64, Jan. 2024.

[15] J. Huang and Y. Zhang, "Essays on conceptual electrochemistry: I. Bridging open-circuit voltage of electrochemical cells and charge distribution at electrode-electrolyte interfaces," *Frontiers in chemistry*, vol. 10, no. 1095988, Nov. 2022.

[16] H. Shu, G. Wang, and X. Tian *et al*., "Single-ended protection method of MMC-HVDC transmission line based on random matrix theory," *International Journal of Electrical Power & Energy Systems*, vol. 142, no. 108299, Nov. 2022.

[17] X. He, C. Lei, and Q. Ai *et al*., "Invisible units detection and estimation based on random matrix theory," *IEEE Transactions Power Systems*, vol. 35, no. 3, pp. 1846-1855, May 2020.

[18] B. Li, Z. Li, and P. Ju, "An edge-cloud collaborative fault detection method for low-voltage distribution networks based on random matrix theory," *Proceedings of the CSEE*, vol. 42, no. 1, pp. 25-36, Jan. 2022. (in Chinese)

[19] H. Shu, Y. Dai, and N. An *et al*., "Fault identification method of MMC-HVDC line based on sequential overlapping derivative transform," *Transactions of China Electrotechnical Society*, vol. 3636, no. 1, pp. 203-214, 226, Jan. 2021. (in Chinese)

[20] Y. Zhao, W. Wang, and S. Yan, "Distributionally robust optimization scheduling of a joint wind-solar-storage system considering step-type carbon trading," *Power System Protection and Control*, vol. 51, no. 6, Mar. 2023. (in Chinese)

[21] S. Zhang, S. Ge, and H. Liu *et al*., "Model and observation of the feasible region for PV integration capacity considering Wasserstein-distance-based distributionally robust chance constraints," *Applied Energy*, vol. 347, no. 121312, Oct. 2023.

[22] A. Luque, M. Mazzoleni, and A. Carrasco *et al*., "Visualizing classification results: confusion star and confusion gear," *IEEE Access*, vol. 10, pp. 1659-1677, Jan. 2022.

[23] P. K. Dash, Eluri N. V. D. V. Prasad, and R. K. Jalli *et al*., "Multiple power quality disturbances analysis in photovoltaic integrated direct current microgrid using adaptive morphological filter with deep learning algorithm," *Applied Energy*, vol. 309, no. 118454, Mar. 2022.

[24] Z. Liu, "Simulation of cell to cell variations and thermal management in lithium-ion battery packs," Ph.D. dissertation, the School of Chemical Engineering and Technology, Tianjin University, Tianjin, China, 2014.

[25] X. Feng, C. Xu, and X. He *et al*., "Mechanisms for the evolution of cell variations within a LiNixCoyMnzO2/graphite lithium-ion battery pack caused by temperature non-uniformity," *Journal of Cleaner Production*, vol. 205, pp. 447-462, Dec. 2018.